Kinetic investigation of hydroxide ion and DNA attack on some high spin iron (II) chelates Bearing ONO Donors amino acid Schiff bases

Laila H. Abdel-Rahman, Rafat M. El-Khatib, Lobna A. E. Nassr and Ahmed M. Abu-Dief
Chemistry Deptartment, Faculty of Science, Sohag University, 82534, Sohag, Egypt

Abstract: The reactivity of few novel high spin Fe(II) complexes of Schiff base ligands derived from 2-hydroxynaphthaldehyde and some variety of amino acids with OH$^-$ ion has been examined in aqueous mixture at temperature in the range 10–40 C^o. Based on the kinetic investigations, the rate law and a plausible mechanism were proposed and discussed. The general rate equation was suggested as follows: rate = k_{obs} [Complex], where $k_{obs.}$ = k_1 + k_2 [OH$^-$]. Base catalyzed hydrolysis kinetics measurements imply pseudo-first-order doubly stage rates due the presence of mer- and fac-isomers. The observed rate constants k_{obs} are correlated the effect of substituent R in the structure of the ligands. From the effect of temperature on the rate; various thermodynamic parameters have been evaluated. The evaluated rate constants and activation parameters are in a good agreement with the stability constants of the investigated complexes.

Introduction

Schiff base complexes have extensive importance as radiotracers [1], biologically active reagents [2–5], catalysts for oxidation [6, 7], epoxidation [8], polymerization [9] and decomposition reactions [10, 11]. On the other hand, considerable attention has been paid over the last few decades in establishing substitution reactions, dissociation, hydroxide attack, and reaction with cyanide of low-spin tris-ligand Fe(II) complexes. Some studies have been carried out on 1,10-phenanthroline complexes [12–14], complexes of substituted 2,2'−bipyridyl [15], complexes of Schiff base ligands derived from pyridine 2-carboxaldehyde [16] or 2-benzoylpyridine [17], and other derivatives [18]. Moreover, substituents effects on reactivity have been considered for base hydrolysis of tris-ligand-Fe(II) complexes of Schiff base ligands derived from 2-acetylpyridine and substituted benzylamines and their aniline analogues [19]. From a bioinorganic point of view, iron Schiff base complexes provide useful structural and electronic models for the similarly coordinated sites found in the heme iron enzymes. Moreover, these complexes are also important for the asymmetric oxidation of organic substrates, since their structure and catalytic activity are analogous with those of iron porphyrins [20]. This contribution deals with the of hydroxide attack on some newly prepared and characterized Schiff base amino acid Fe(II) complexes [21]. The particular importance of the ligands used in this study (Scheme 1) is their sufficiently strong interaction with Fe(II) central metal Kinetic data concerning the base hydrolysis reaction of the important Fe(II) Schiff base amino acid complexes will help to complete the scan of pH effects on the reactivity of these vital complexes and subsequently will be very helpful in extending their applications. Substituent, temperature and pH effects on the reactivity of these important chelates of wide applications have long been ignored and chemists worldwide would be greatly interested in these kinetic data.

386

Materials and methods

The iron (II) complexes were prepared according to elsewhere [21, 22]. An aqueous solution of the α-amino acid was mixed with a hot ethanolic solution of the aldehyde in stoichiometric amounts. The resulting amino acid Schiff base ligand was then stabilized by chelation to iron(II) by adding an aqueous solution of ferrous ammonium sulfate in an equivalent ratio. To avoid the Fe(II) oxidation, five to six drops of glacial acetic acid were added. The resulting solution was stirred magnetically for 9 h with continuous N_2 bubbling. The isolated complexes were recrystallized from water–ethanol solutions. The composition of the complexes was established by CHN microanalysis, IR, UV–vis spectral analyses, magnetic moment and conductivity measurements. Full details of characterization of the present complexes can be found in our previous publication and all gave satisfactory data [21]. All applied analyses have been consistent with their proposal structures. The purity of these complexes was checked spectrophotometrically (cf. Table I), by confirming that the kinetics were exactly first-order up to 90% of the reaction progress, and that the obtained rate constants agreed well with the reported values. We have tested the solutions, over a long period of time, at least a month, for the stability of Fe(II) cation by their resistance toward reduction with dithionite. Again, if an aged complex solution was treated with NaOH under N_2, a green precipitate of $Fe(OH)_2$ formed, indicating the presence of Fe(II) in the complex solution used in the kinetic runs. It was observed that in these runs, the intense violet color of the complex solution fades during the course of each reaction. The solution then turns colorless and some trace green colloidal particles of $Fe(OH)_2$ turning pale yellow appear. Finally, the hydrolysis product precipitates as brown $Fe(OH)_3$ by oxidation with O_2 dissolved in solution long after the end of the kinetic run. Sodium hydroxide (99.3%), sodium nitrate (99%) and oxalic acid (99.7%) were obtained from BDH.

Kinetic experiments were carried out by following the decrease in absorbance at λ_{max}, the absorption maximum of the investigated complexes, in a Jasco UV-Visible spectrophotometer V-530 with 10 mm matched quartz cells connected with an ultrathermostate (CRIOTERM model 190) water circulator over the first 2.5 half lives for each run [23-25]. It was confirmed that there was no interference from any other reagents at this wavelength (Fig. 2). The reactants, i.e., the complex and sodium hydroxide, were mixed so that the reaction obeyed pseudo-first-order kinetics, where $[OH^-] \gg [complex]$. The pseudo-first-order constants were computed by means of a least-mean-squares program from the slopes of the first-order plots and reported in Table (2). The two-stage kinetics obtained from these plots was explained as due to the presence of the convenient labile cis and inert trans isomers of the octahedral structures [26] (cf. Fig. 4). Standard analysis of the absorbance versus time plots gave satisfactory estimates for the slow second-stage rate constant values reported in table 2. The concentration of sodium hydroxide was determined by using usual analytical method with standard oxalic acid. The ionic strength of the solution was kept constant at 0.01 M using sodium nitrate. Tthe activation parameters were calculated from Arrhenius and Eyring plots (T =283– 313 K).

Kinetic study of the interaction of the investigated complexes with DNA

The interaction of the prepared complexes with calf thymus DNA was kinetically studied on PG UV-Visible spectrophotometer at 25.0 ± 1 ℃.

Results and discussion

The characteristic band for the investigated com-plexes in the UV/visible spectra lies at $\lambda_{max} = 494$ - 520 nm (cf. table 1). But on addition of the base, a red shift occurred at 518 nm. Then, this new band decays by first-order kinetics in [complex].

Repeated spectral scans (cf. Fig. 2) show first-order kinetics of the base fission of the attacked complex intermediate. The base hydrolysis reaction of the investigated complexes is simply a nucleophilic attack of OH^- ion at the complex, which affords free ligand, and in the presence of the dissolved oxygen in the solution, colloidal Fe(III) hydroxide. The cell contents are yellow and optically clear at the end of each run. All the complexes gave evidence for two-stage kinetics. Standard analyses of the absorbance vs. time traces presented good estimates for the fast and slow stages (cf. Fig. 3). It is assumed that the first stage corresponds to the parallel base hydrolysis reactivity of more labile isomer that is expected to be fac and inert mer forms, and the second stage corresponds to the reactivity of mer inert form only, as has been observed elsewhere [26] (cf. Schemes 2, 3). Vichi and Krumholz reported kinetics for aquation of the iron(II) complexes derived from pyridine-2-carboxaldehyde and n-propylamine. They interpreted their results in terms of parallel first-order processes associated with the break of the two different iron–nitrogen bonds at sufficiently different rates of mer and fac isomers [27], which are in thermodynamically equilibrium in solution. In the reported investigation [28], the contribution from the first step readily became smaller if a stock solution of the complex was allowed to stand for increasing periods of time because of hydrolysis of labile isomer. In our investigated complexes, the fast isomer remains for longer periods compared with those complexes investigated elsewhere [28].

Reaction mechanism of hydroxide ion attack on Iron(II) chelates

First-order rate constants for the base hydrolysis reactions (k_{obs}) in aqueous media are cited in Table 2. The plots of k_{obs} against hydroxide concentration exhibited linear curves (cf. Fig. 3). The general rate law used in the case of wide ranges of hydroxide concentrations and ionic strengths

$$Rate = \frac{-d[complex]}{dt} = (k_1 + k_2[OH^-])[complex] \quad (1)$$

where k_1 is the rate constant of dissociation of the complex in neutral solution. In the presence of hydroxide concentrations employed in this contribution, only the $k_2[OH^-]$ term is usually significant [29], and the observed linear k_{obs} dependences on hydroxide ion concentration obey the following equation:

$$k_{obs} = k_1 + k_2[OH^-] \quad (2)$$

The values of first k_1 and second k_2 order rate constants were evaluated by least square of k_{obs} with $[OH^-]$ and cited in table 3. It was found that the values of the observed rate constants k_{obs} are correlated the effect of substituent R in the structure of the complexes under investigation. The order of reactivity of the prepared complexes towards the hydroxide attack is increased in the sequence: nari < nali < nphali < nasi < nhi. Thismay be rationalized to the inductive effect of the substituent.

388

The suggested mechanism for the base hydrolysis reaction of the investigated complexes was given the following scheme:
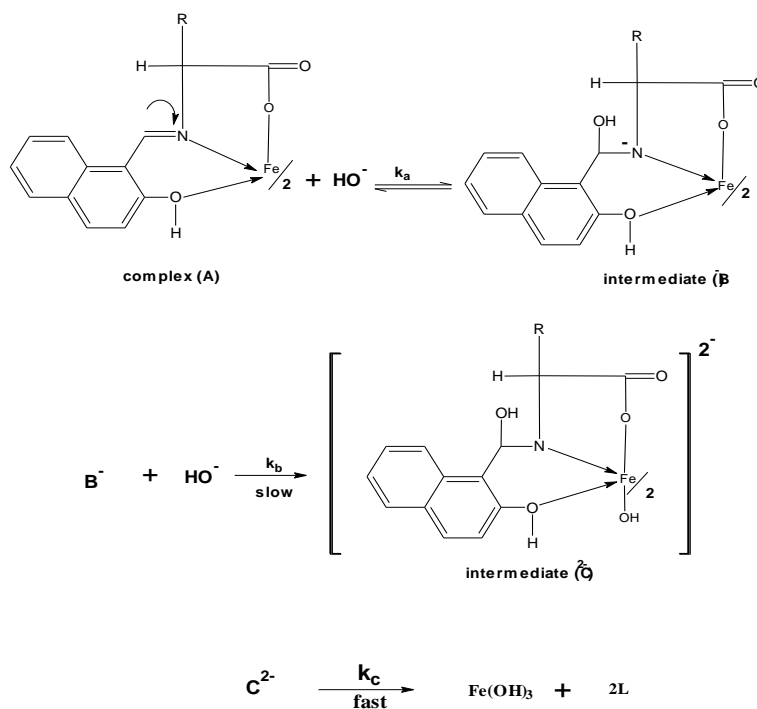
The proposed mechanism, for which there are precedents in ruthenium(II) chemistry [27], assumes a fast pre equilibrium step in which one hydroxide ion attacks the electrophilic azomethine carbon atom [30] to form the intermediate B^{2-}. Furthermore, it is suggested that the rate-determining step implies the parallel attack of the hydroxide ion on the central iron atom in the intermediate B^{2-} giving the intermediate C^{3-} and the liberation of the first ligand. The high electron density of the t_2g^6 configuration [31] of Fe(II) in the octahedral chelates would make the attack of hydroxide ion on the iron atom difficult.

Based on this mechanism, the base hydrolysis reaction rate can be derived by applying the steady-state approximation for the concentrations of the intermediates, as follows:

$$Rate = \frac{-d[complex]}{dt} = \frac{k_a k_b k_c [OH^-][A]_T}{1 + k_a k_b [OH^-] + k_a k_c [OH^-]} \qquad (3)$$

where $[A]_T$ is the total analytical concentration of the complex,

$$k_{obs} = \frac{k_a k_b k_c [OH^-]}{1 + k_a k_b [OH^-] + k_a k_c [OH^-]} \qquad (4)$$

389

To obtain more details about the recent $$[A_T] = [A^-]_{ss} + [B^-]_{ss} + [C^{2-}]_{ss} \quad (5)$$ reaction mechanism, the value of the reaction order (n) for [OH$^-$] was determined by a least squares procedure from the slopes of the linear plots of ln (k_{obs}- k_1) vs. ln [OH$^-$] cf. Figs.(5) according to the following equation:

$$\ln(k_{obs} - k_1) = \ln k_2 + n \ln [OH^-] \quad (6)$$

The values of n were found to be in the range from 0.759 to 1.013 for the different investigated complexes.

Figure 6 shows the dissociation curves for the studied complexes. The absorbance values of these complexes, in different aqueous buffer media, were monitored after an average time of 48 h. Thus these curves elucidate that in the solutions of pH range 4 – 10, the tested complexes are stable and inert against the hydroxide attack. This result is confirmed by the extremely low k_1 values, the dissociation rate constant in the aqueous neutral, weak acidic and alkaline solutions for the investigated complexes. The maintenance of the intensely violet colored solutions of our complexes in the pH range 4–10, over enough average time (48 h) gives a visual appreciation of their stabilities in these solutions. This confirms the suggested mechanism since at pHs > 9, the rate of base hydrolysis increases with increasing pH. The data in Table 3 reveals that the relative reactivity trends for our Fe(II) complexes are mainly controlled by hydrophobic and hydrophilic characters of these complexes. As hydrophobicity increases, rate of the reaction decreases. This is ascribed to the destabilization of the more hydrophobic transient species [30] on one hand, and the opposing stabilization of hyroxide in the aqueous media on the other hand. This explains the observed highest values of the reaction rate for nasi with much less hydrophobic character, and the lowest reported values for nari with the most hydrophobic entity.

Determination of thermodynamic parameters

The activation parameters for the base hydrolysis reaction were calculated, for the investigated complexes by least squares determination of slopes and intercepts of Arrhenius and Eyring plots (cf. Figs. 7, 8] and collected in Table 4. It is of interest that the pK values calculated for the investigated complexes are in agreement with the kinetic and activation parameters. The higher the pK values, the stability constant of the complexes, the lower the reactivity against hydroxide attack and thus the greater the activation energy for the reaction was observed, cf. Table 4. The pK values of the complexes were determined by the spectrophotometric continuous variation method [21]. The potentiometric method was tried but failed due to the precipitation of iron hydroxide, as well as the difficulty in preparing amino acid Schiff bases as solids.

It is worth mentioning that the activation parameters are important for determination of the reaction rate and mechanism From Table 4, the high, negative values of the entropy of activation support the proposed mechanism that the investigated reaction takes place via the formation of an intermediate complex [24, 25]. It is interesting that the different thermodynamic functions are consistent in their trends.

As entropy of activation ($\Delta S^{\neq}$) increases, changing to less negative values, the rate constant decreases, and activation energy increases. This behavior can be ascribed to enhancing stability of activated complex intermediate.

Reactivity of the investigated complexes to DNA

The repeated spectral scans of the reaction between DNA and the investigated complexes is characterized with formation of isosbestic points which confirm that the reaction between them (cf. Fig. (9)), The values of observed rate constants of that reaction were calculated by the least squares of absorbance with time (cf. Fig. 10 and Table 5)

The values of observed rate constants were correlated with the reported binding constants of the interaction of the investigated Schiff base amino acid Fe (II) complexes with DNA [our reference]. It was found that the reactivity of the investigated complexes towards DNA is in a good agreement with the reported binding constants. The reactivity of the prepared complexes towards DNA are increasing in the following order nari < nphali < nali < nasi < nhi

The rate constant k_{obs} values for the interaction between CTDNA and the investigated complexes were calculated by plotting –log A versus time (cf. Table 5). The plot of k_{obs} versus[DNA] gave a straight line suggesting a pseudo-first order reaction kinetics (cf. Fig.10).

The second order rate constant values for the reaction between CT-DNA and the investigated complexes were calculated from the least square of k_{obs} with [DNA] and also found to be in a good agreement with binding constant values (cf. Table 5).

Linear plots of $k_{obs.}$ against [DNA] were schemed in Figs. (10) and are in a good correlation with the following equation:

$$Rate = -\frac{d[complex]}{dt} = k_{obs}[complex] \qquad (7)$$

The overall rate law for the investigated reaction under the adopted conditions of pseudo first order kinetics can be represented as follows:

$$Rate = k_{obs}[complex] = (k_1 + k_2[DNA])[complex] \quad (8)$$

The k_1 term is assigned to rate determining dissociation of the investigated complexes and the k_2 term to rate determining attack by DNA at the compounds, where $k_{obs} = k_1 + k_2$ [DNA].

Determination of reaction order

The value of the reaction order (n) for [DNA] was determined by a least squares procedure from the slops of the linear plots of ln ($k_{obs\,-}$ k_1) vs. ln [DNA] (cf. Figs. 11) according to the following equation:

$$\ln (k_{obs} - k_1) = \ln k_2 + n \ln [DNA] \qquad (9)$$

391

The values of n were recorded in Table (6). Table 8 shows that the reaction between CT-DNA and the investigated complexes follow first order kinetics in respect of [DNA].

References
1. H. Luo, P. E. Fanwick, M. A. Green, Inorg. Chem. 37 (1998) 1127.
2. G. G. Mohamed, M. M. Omar, A. M. M. Hindy, Spectrochim. Acta A 62 (2005) 1140.
3. M. El-Behery, H. El-Twigry, Spectrochim. Acta A 66 (2007) 28.
4. Z. Afrasiabi, E. Sinn, W. Lin, Y. Ma, C. Campana, S. Padhye, J. Inorg. Biochem. 99 (2005) 1526.
5 N. Raman, A. Kulandaisamy, C. Thangaraja, Trans.Met. Chem. 29 (2004) 129.
6. H. S. Abbo, S. J. J. Titinchic, R. Prasad, S. Chand, J. Mol. Catal. A: Chem. 225 (2005) 225.
7. K. C. Gupta, A. K. Sutar, J. Mol. Catal. A: Chem. 272 (2007) 64.
8. H. Shyu, H. Wei, G. Lee, Y. Wang, J. Chem. Soc., Dalton Trans. 915. (2000).
9. Z. Wu, D. Xu, Z. Feng, Polyhedron 20 (2001) 281.
10. M. Nath, S. Kamaluddin, J. Cheema, Ind. J. Chem. 32A (2) (1993) 108.
11. K. C. Gupta, H. K. Abdulkadir, S. Chand, J. Mol. Catal. A : Chem. 202 (2003) 253.
12. Burgess, J.; Prince, R. H. J Chem Soc 1963, 5752.
13. Burgess, J. J Chem Soc (A) 1967, 431; (b) Burgess, J. Inorg Chim Acta 1971, 5, 133.
14. Burgess, J.; Prince, R. H. J Chem Soc 1965, 4697.
15. Burgess, J.; Prince, R. H. J Chem Soc 1965, 6061.
16. Burgess, J.; Prince, R. H. J Chem Soc (A) 1965, 434.
17. Burgess, J. J Chem Soc (A) 1968, 497.
18. Krumholz, P. Struct Bonding 1971, 9, 139.
19. Alshehri, S.; Burgess, J.; Shaker, A. M. Trans Met. Chem. 1998, 23, 689..
20. Canali, L.; Sherrington, D. C. Chem Soc Rev 1999, 28, 85.
21. Laila H. Abdel-Rahman, Rafat M. El-Khatib, Lobna A. E. Nassr and Ahmed M. Abu-Dief, J. Mol. Str., accepted 19-2-2013
22. Sharm, P. K.; Dubey, S. N. Indian J Chem 1994, 33A (12), 1113.
23. Abu-Gharib, Ezz. A., EL-Khatib, Rafat. M., Nassr, Lobna A. E. and Abu-Dief, Ahmed M., 2011. Z. Phys. Chem. 225, 1.
24. Abu-Gharib, Ezz. A., EL-Khatib, Rafat. M., Nassr, Lobna A. E. and Abu-Dief, Ahmed M., 2011. J. Korean chem. Soc. 50, 3, 346.
25. Abu-Gharib, Ezz. A., EL-Khatib, Rafat. M., Nassr, Lobna A. E. and Abu-Dief, Ahmed M. Kinetics and Catalysis, 2012, Vol. 53, No. 2, pp. 182–187
26. Blandamer, M. J.; Burgess, J.; Elvidge, D. L.; Guardado, P.; Hakin, A. W.; Prouse, L. J. S.; Radulovic, S.; Russell, D. R. Transition Met Chem 1991, 16, 82.
27. Vichi, E. J. S.; Kurmholz, P. J Chem Soc, Dalton Trans 1975, 1543.
28. Alshehri, S.; Burgess, J.; Shaker, A. M. Trans Met Chem 1998, 23, 689.
29. Blandamer, M. J.; Burgess, J.; Coohson, P.; Roberts, D. L.; Willings, P.; Mekhail, F. M.; Askalani, P. J Chem Soc, Dalton Trans 1978, 996.
30. Alshehri, S.; Blandamer, M. J.; Burgess, J.; Guardado, P.; Hurbbard, C. D. Polyhedron 1993, 12(5), 445.
31. Burgess, J.; Ellis, G. E.; Evans, D. J.; Porter, A.; Wane, R.; Wyvill, R. D. J Chem Soc (A) 1971, 44–48.